International Journal of Applied Mathematics

Volume 27 No. 1 2014, 109-119
ISSN: 1311-1728 (printed version); ISSN: 1314-8060 (on-line version)
doi: http://dx.doi.org/10.12732/ijam.v27i1.10

SMOOTH SPLINE BLENDING SURFACE APPROXIMATION OVER A TRIANGULATED IRREGULAR NETWORK

Rune Dalmo[1] §, Jostein Bratlie[2], Børre Bang[3], Arne Laksås[4]

Faculty of Technology
Narvik University College
P.O. Box 385, 8505 Narvik, NORWAY

Abstract: A Triangulated Irregular Network (TIN) is a data structure commonly used to represent a geometric surface in computer software systems, such as geographic information systems and terrain modeling systems. Expo-rational B-splines (ERBS), a blending type spline construction in the family of generalized expo-rational B-splines (GERBS), can be used to create an approximation surface which interpolates the vertex positions of the TIN nodes. Utilizing the properties for local support of this blending spline construction, one can construct an approximation surface which is local within the second neighbourhood with respect to the infliction nodes of the underlying TIN. We present two variations of blending functions used with the construction. The first one blends the TIN edges with a smooth component, thus, the surface approximation is only C^0 over the TIN edges. The second blending method provides a surface approximation which is smooth over the TIN edges.

AMS Subject Classification: 65D05, 65D07, 65D10
Key Words: triangulated irregular network, approximation, blending, expo-rational B-spline

1. Introduction

Various methods for approximation and interpolation to obtain visually nice, or smooth, surfaces have been explored to the present. We provide here a brief

Received: January 31, 2014

§Correspondence author

overview of some blending methods applicable to arbitrary triangulations of non-regular data.

Triangular Bernstein-Bézier patches, described e.g. in [3], can be joined together smoothly by constructing pairs of co-planar triangles. However, the conditions ensuring a sufficient continuity across the common boundary lock triangles together and the construction becomes stiff. Besides, the number of co-planar triangles required grows with increasing degree of continuity, making the construction less local.

Schumaker et al. explored methods in [12, 6] where they utilize spline functions on macro-element spaces. Macro-elements of required smoothness are constructed on splits of triangles. They are used to construct super-spline spaces with local, stable bases, to overcome the above mentioned problems.

The parameterization method of [4] by Floater, although it is not a blending type method, is applicable to smooth surface approximation of triangulations, notably using the shape-preserving parameterization [4] or mean value coordinates [5].

Techniques based on radial basis functions, introduced by Broomhead and Lowe in the neural network community [1], are now common tools for geometric data analysis. We note here that triangular data structures, since they define connectivity between vertices, can be used to determine constraints for radial basis functions. Thus, blending of radial basis functions can be considered to construct smooth surface approximations over triangulations.

In this paper we describe, using expo-rational B-spline (ERBS) surfaces [8], blending over a triangulation based on non-regular data. Our motivation is to generate a surface which is smooth over the TIN edges and at the same time interpolates the vertex positions.

The following sections explain the kind of triangulations we consider, ERBS patches and how they are constructed from pairs of triangles, how we approximate, do interpolation and blend the results, followed by some examples.

2. Preliminaries

2.1. Triangulated Irregular Network

The triangulated irregular network (TIN), proposed and explored by Peucker et al. in a series of papers, notably [10, 11], is a digital terrain model (DTM) consisting of irregularly distributed nodes and lines. It constitutes a network of non-overlapping triangles representing a tessellation of a surface, usually in

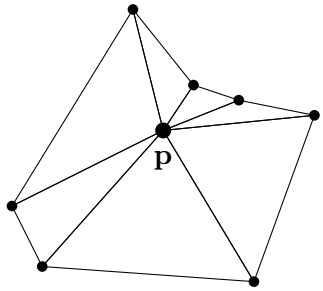

Figure 1: A point **p** and its first neighborhood (points connected to this point through an edge) in a TIN

Euclidean space $\mathbb{R}^3$. TINs are typically vector-based representations of terrain data. They are commonly used in geographical information systems (GIS). The TIN surface model is oriented to line features as well as points. Using triangles to represent terrain facilitates a realistic representation if the spatial data units recognize natural surface changes in slope, at peaks, pits, passes, ridge lines, saddle points and course lines or discontinuities. Triangular facets can be created to meet these conditions by having their corners located at control points with exact known coordinates, and having triangle edges fall along approximations of ridges. More information regarding terrain representation based on TINs can be found in [9].

A part of a TIN is displayed in fig. 1. Due to the nature of TIN data we conclude that it is possible to "see" the first neighborhood from any point in a TIN and measure the distances along the edges. Using this it follows that an edge does not intersect the physical terrain.

2.2. Expo-Rational B-Splines

Expo-rational B-splines, as defined in [8], provide a blending type construction where local functions at each knot are blended together by C^∞-smooth basis functions:

$$f(t) = \sum_{k=1}^{n} l_k(t) B_k(t) \tag{1}$$

where $\mathbf{t} = \{t_k\}_{k=0}^{k=n+1}$ is an increasing knot vector, and each basis function $B_j(t)$ is C^∞ on its support (t_{j-1}, t_{j+1}) with $B_k(t_k) = 1$, and $D^j B_k(t_k) = 0$ for $j = 1, 2, \ldots$.

In this paper we consider the scalable subset of the ERBS basis presented

in [2] with the default set of intrinsic parameters proposed by Laksås in [7]:

$$B_k(t) = \begin{cases} S_{k-1} \int_0^{w_{k-1}(t)} \psi_{k-1}(s)ds, & t_{k-1} < t \leq t_k \\ S_k \int_{w_k(t)}^1 \psi_k(s)ds, & t_k < t < t_{k+1} \\ 0, & \text{otherwise,} \end{cases} \tag{2}$$

where $w_k(t) = \frac{t-t_k}{t_{k+1}-t_k}$, $\psi(t) = e^{-\frac{\left(t-\frac{1}{2}\right)^2}{t(1-t)}}$, and $S_k = \left(\int_0^1 \psi_k(t)dt\right)^{-1}$.

We have the following general formula for parametric tensor product surfaces using ERBS,

$$S(u,v) = \sum_{i=1}^{n_u} \sum_{j=1}^{n_v} s_{ij}(u,v) B_i(u) B_j(v), \tag{3}$$

where $s_{ij}(u,v),\ i = 1,\ldots,n_u,\ j = 1,\ldots,n_v$ are $n_u \times n_v$ local Bézier surface patches, and $B_i(u), B_j(v)$ are the respective ERBS basis functions.

3. ERBS over a TIN

Given a TIN, $\Delta(x,y,z)$, which is a tessellation of a surface in $\mathbb{R}^3$ where the z axis represents data, for instance physical terrain heights. We construct ERBS surface patches from pairs of neighboring triangles by considering inner edges in the TIN structure. Each ERBS surface patch $L(u,v)$ is a differentiable map, $L : \mathbf{\Omega}_L \subset \mathbb{R}^2 \to \mathbb{R}^3$. Figure 2a illustrates an ERBS surface patch construction, based on four bi-linear Bézier local surfaces, as defined in eq. (3). Its positions $\mathbf{p}_i,\ i = 1,\ldots,4$ and derivatives $\mathbf{u}_1, \mathbf{u}_2, \mathbf{v}_1$ and $\mathbf{v}_2$ are retrieved from the triangulation, where $\mathbf{p}_1, \mathbf{p}_2$ and $\mathbf{p}_3$ are vertices in one triangle, and $\mathbf{p}_1, \mathbf{p}_3$ and $\mathbf{p}_4$ outline a neighbor triangle. The dotted line between $\mathbf{p}_1$ and $\mathbf{p}_3$ constitutes the common edge shared by the two triangles. Figure 2b illustrates an ERBS surface patch on a TIN.

Directional derivatives for the bi-linear Bézier local surface $S(u,v)$ in position $\mathbf{p}_1$ are defined as follows:

$$\begin{aligned} \frac{\partial S}{\partial u} &= \mathbf{p}_2 - \mathbf{p}_1, \\ \frac{\partial S}{\partial v} &= \mathbf{p}_4 - \mathbf{p}_1, \\ \frac{\partial^2 S}{\partial u \partial v} &= (\mathbf{p}_3 + \mathbf{p}_1) - (\mathbf{p}_4 + \mathbf{p}_2). \end{aligned} \tag{4}$$

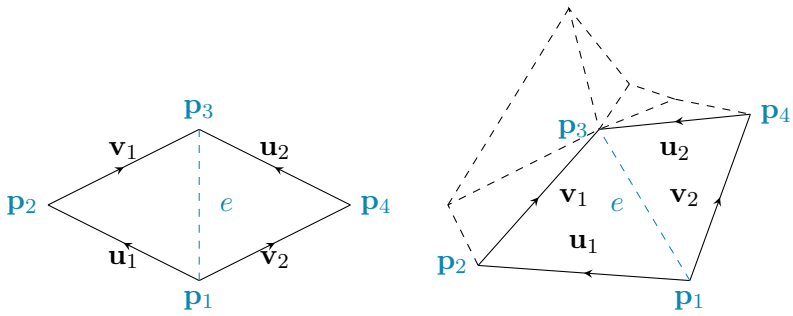

(a) An ERBS surface patch $L(u, v)$

(b) An ERBS surface patch $L(u, v)$ on a TIN $\Delta(x, y, z)$

Figure 2: Bi-linear ERBS surface patches constructed from vertices and edges in two neighboring triangles.

Directional derivatives for the three remaining Bézier surfaces local to one ERBS surface patch, one in each of the vertices $\mathbf{p}_2$, $\mathbf{p}_3$ and $\mathbf{p}_4$, are defined in a manner similar to eq. (4).

A consequence of the ERBS Hermite interpolation properties explored in [7, theorem 2.4] is that the derivatives of an ERBS surface patch, in a given knot, are equal to all existing derivatives of the Bézier local surface in that knot. It follows that each ERBS surface patch interpolates TIN positions in four vertices: $\mathbf{p}_1, \mathbf{p}_2, \mathbf{p}_3$ and $\mathbf{p}_4$ in fig. 2.

4. Smooth Surface Construction

We define a parametric regular grid surface $\Theta(u, v)$, $\Theta : \mathbf{\Omega}_\Theta \subset \mathbb{R}^2 \to \mathbb{R}^3$, which covers the triangulation $\Delta(x, y, z)$. The positions in $\mathbb{R}^3$ for the points $\mathbf{p}_\Theta(u, v)$ on the surface Θ are computed as follows. First we find in which triangle $t \in \Delta$ the point $\mathbf{p}_\Delta$ is inside, where $\mathbf{p}_\Delta$ is a 2D projection of $\mathbf{p}_\Theta$ mapped to Δ in Cartesian coordinates. Next, we evaluate each ERBS surface patch L_i in $\mathbf{p}_{L_i}$, where L_i covers t and $\mathbf{p}_{L_i}$ is $\mathbf{p}_\Theta$ mapped to L_i in its local coordinates, and blend the results. We denote the mapping from $\mathbf{p}_\Theta$ to $\mathbf{p}_{L_i}$ by $\omega_i(u, v)$.

The blending distribution is computed from the barycentric coordinates of the triangles. We present two blending functions, which are both invariant under affine maps, utilizing the scalable subset of the ERBS basis function.

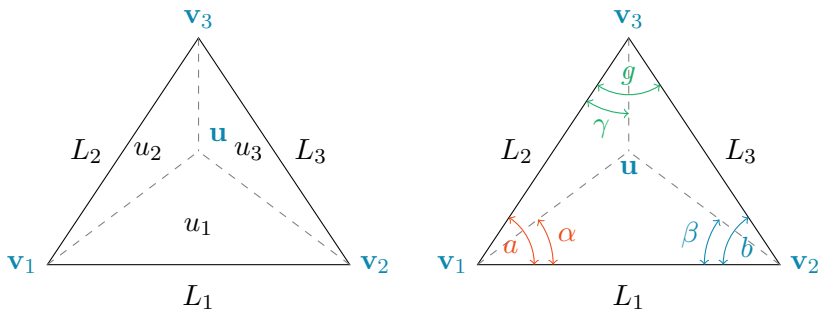

(a) Using homogeneous barycentric coordinates u_1, u_2 and u_3.

(b) Using angle ratios $\frac{\alpha}{a}$, $\frac{\beta}{b}$ and $\frac{\gamma}{g}$.

Figure 3: Bi-linear ERBS surface patches constructed from vertices and edges in two neighboring triangles.

4.1. Blending using Custom ERBS Triangles

A set of ERBS basis functions in homogeneous barycentric coordinates is defined in [7] as

$$\mathcal{B}_{k,i}(\mathbf{u}) = \frac{B(u_i)}{\sum_{j=1}^{k} B(u_j)} \text{ for } k > 1 \text{ and } i = 1, 2, \ldots, k, \tag{5}$$

and where $B(u_i)$, $i = 1, 2, \ldots, k$ is defined in eq. (2). In the case of triangles, each $\mathcal{B}_{3,i}(\mathbf{u})$ evaluates to 1 in the vertex u_i and 0 in the two other vertices. Everywhere else the value is between 0 and 1.

ERBS surface patches can be blended using a slightly modified version of the ERBS triangle in eq. (5). Given a point $\mathbf{u} = (u_1, u_2, u_3)$, in homogeneous barycentric coordinates, as shown in fig. 3a. Then

$$\Theta(u, v) = \sum_{i=1}^{3} \hat{\mathcal{B}}_i(\mathbf{u})\ L_i \circ \omega_i(u, v), \tag{6}$$

where $L_i \circ \omega_i(u, v)$ is the ith ERBS surface patch evaluated in its local coordinates, and the set of ERBS basis functions $\hat{\mathcal{B}}_i(\mathbf{u})$ is defined as

$$\hat{\mathcal{B}}_i(\mathbf{u}) = \frac{B(1 - u_i)}{\sum_{j=1}^{3} B(1 - u_j)},\ i = 1, 2, 3, \tag{7}$$

where we clearly can see that $\sum_{i=1}^{3} \hat{\mathcal{B}}_i(\mathbf{u}) = 1$.

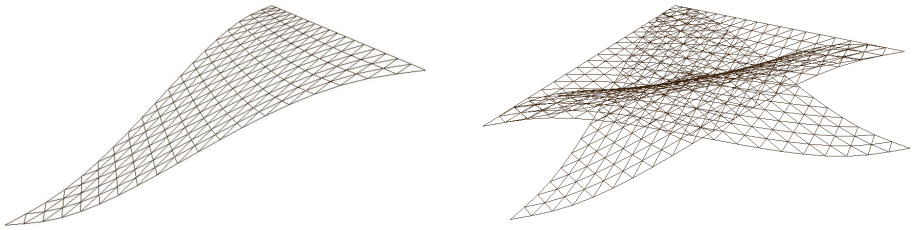

(a) One ERBS basis function $\hat{\mathcal{B}}_i(\mathbf{u})$. It evaluates to 0 in one vertex, $\frac{1}{2}$ along the opposing edge and between 0 and $\frac{1}{2}$ elsewhere.

(b) Three modified ERBS triangles $\hat{\mathcal{B}}_i(\mathbf{u})$, $i = 1, 2, 3$ in homogeneous barycentric coordinates. The sum of the basis functions is 1 everywhere.

Figure 4: Modified ERBS triangles in homogeneous barycentric coordinates, rendered with triangle strips. The plots do not show parameter lines.

A plot of the modified ERBS triangle in eq. (7) is shown in fig. 4a. It evaluates to 0 in one vertex, is positive on the edges, is $\frac{1}{2}$ along the opposing edge between the two other vertices and is between 0 and $\frac{1}{2}$ elsewhere. As a consequence, when it comes to blending of ERBS surface patches on a specific edge, we conclude that one ERBS triangle is $\frac{1}{2}$ and the two other ERBS triangles sum up to $\frac{1}{2}$. Figure 4b illustrates this by showing three modified ERBS triangles in homogeneous barycentric coordinates.

4.2. Blending using Angle Ratios in Triangles

Given a point $\mathbf{u} = (u_1, u_2, u_3)$, in homogeneous barycentric coordinates, as shown in fig. 3b. Then

$$\begin{aligned}\Theta(u,v) = \Big(\Big(1 - B\left(\tfrac{\alpha}{a}\right)\Big)\ L_1 \circ \omega_1(u,v)\ + \\ B\left(\tfrac{\alpha}{a}\right)\ L_2 \circ \omega_2(u,v)\Big)\ \Big(1 - B\left(\tfrac{\gamma}{g}\right)\Big) \\ + \Big(\Big(1 - B\left(\tfrac{\beta}{b}\right)\Big)\ L_1 \circ \omega_1(u,v)\ + \\ B\left(\tfrac{\beta}{b}\right)\ L_3 \circ \omega_3(u,v)\Big)\ B\left(\tfrac{\gamma}{g}\right), \end{aligned} \tag{8}$$

where a, b, g, α, β and γ are the angles in fig. 3b, so that α, β and γ depend on $\mathbf{u}$, and $B(u)$ is the ERBS basis function in eq. (2) and $L_i \circ \omega_i(u, v)$ is the ith ERBS surface patch evaluated in its local coordinates. By re-arranging eq. (8)

and using eq. (6) we obtain

$$\begin{aligned}
\tilde{\mathcal{B}}_1(\mathbf{u}) &= \left(1 - B(\tfrac{\alpha}{a})\right)\left(1 - B(\tfrac{\gamma}{g})\right) + \left(1 - B(\tfrac{\beta}{b})\right) B(\tfrac{\gamma}{g}), \\
\tilde{\mathcal{B}}_2(\mathbf{u}) &= B(\tfrac{\alpha}{a})\left(1 - B(\tfrac{\gamma}{g})\right), \\
\tilde{\mathcal{B}}_3(\mathbf{u}) &= B(\tfrac{\beta}{b})B(\tfrac{\gamma}{g}).
\end{aligned} \tag{9}$$

It follows that $\sum_{i=1}^{3} \tilde{\mathcal{B}}_i(\mathbf{u}) = 1$ since

$$\begin{aligned}
\sum_{i=1}^{3} \tilde{\mathcal{B}}_i(\mathbf{u}) = 1 - B(\tfrac{\gamma}{g}) - B(\tfrac{\alpha}{a}) + B(\tfrac{\alpha}{a})B(\tfrac{\gamma}{g}) + B(\tfrac{\gamma}{g}) - B(\tfrac{\beta}{b})B(\tfrac{\gamma}{g}) \\
+ B(\tfrac{\alpha}{a}) - B(\tfrac{\alpha}{a})B(\tfrac{\gamma}{g}) \\
+ B(\tfrac{\beta}{b})B(\tfrac{\gamma}{g}) \\
= 1.
\end{aligned} \tag{10}$$

Figure 5a shows a plot of one of the basis functions in eq. (9). It evaluates to 0 along two edges and 1 along the third edge, but is 1 at one vertex only. Hence, there is a "jump" between basis functions in the vertices.

Using this and investigating eqs. (8) to (10) we conclude that, in this case, one single ERBS surface patch $L_i \circ \omega_i(u, v)$ (see fig. 2a) will be evaluated on each edge. Figure 5b shows a plot of the three basis functions in eq. (9) in homogeneous barycentric coordinates.

5. Concluding Remarks

The method presented in this article is considered to be data-driven. We believe it makes sense to use such methods in cases where we must rely on topology information to generate derivatives. The method is local within the second neighborhood of a TIN node as a consequence of the ERBS surface patch construction.

Whether the construction provides smoothness in the vertices or on the edges depends on the blending functions. The provided blending functions interpolate the position in every vertex. First order directional derivatives, in a given vertex, exist but are not continuous since the limits from the different ERBS surface patches do not converge towards the same. We consider the construction to be C^0 in the vertices.

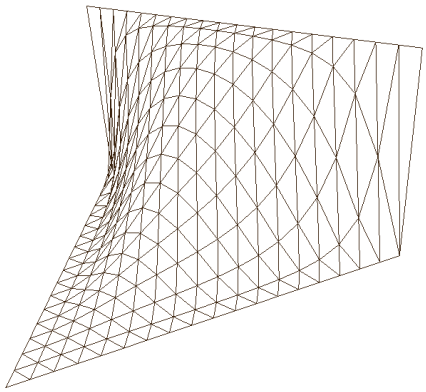

(a) One angle ratio ERBS basis function $\tilde{\mathcal{B}}_i(\mathbf{u})$. It evaluates to 0 along two edges and 1 along one edge.

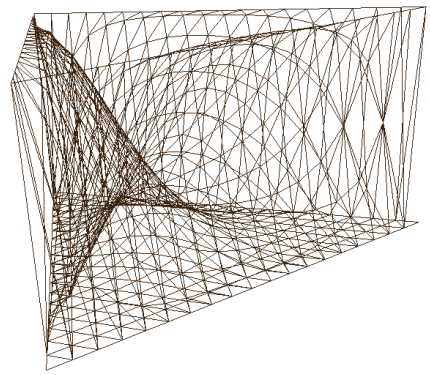

(b) Three angle ratio ERBS basis functions $\tilde{\mathcal{B}}_i(\mathbf{u}), i = 1, 2, 3$. The sum of basis functions is 1 everywhere. On each edge, one basis function evaluates to 1, whereas the two remaining basis functions evaluate to 0.

Figure 5: ERBS blending functions using angle ratios, in homogeneous barycentric coordinates, rendered with triangle strips. The plots do not show parameter lines.

Blending using the original ERBS triangles proposed in [7] (see eq. (5)) provides C^0 approximation over the edges, but is C^∞-smooth in the vertices. In the case of modified ERBS triangles, defined in eq. (7), the resulting surface $\Theta(u, v)$ is C^0 in the vertices and across the edges. However, when compared to the original TIN, the visual result is slightly improved in terms of smoothness, since the ERBS surface patch which is smooth over the considered edge is given the weight $\frac{1}{2}$. "Remains" of edges are still visible due to the jump in first order directional derivatives between the two other patches.

The blending method based on angle ratios, described in eq. (8), ensures that only one ERBS surface patch, which is smooth over the considered edge, is evaluated on that edge. Notably, the surface $\Theta(u, v)$ inherits smoothness properties from the ERBS surface patch over an edge, as a consequence of the ERBS Hermite interpolation properties, since the derivatives of eq. (8) are 0 along the edges (eq. (9)). As expected, the discontinuities in the first order directional derivatives are not longer visible.

We note that there is a trade-off between approximation error and smoothness over edges. The bi-linear Bézier local patches in eq. (4) approximate the

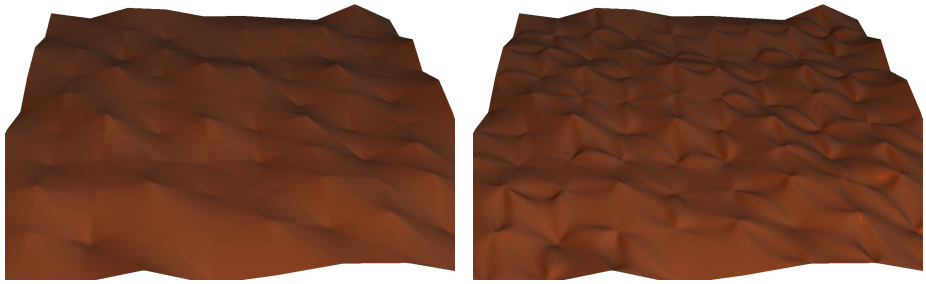

(a) Custom ERBS triangle blending functions. The surface is C^0 across the edges.

(b) ERBS angle ratio blending functions. The surface is smooth across the edges.

Figure 6: Regular grid approximations of a synthetic TIN using different blending methods. TIN vertex positions are interpolated in both cases. The surfaces are C^0 in the vertices and smooth outside vertices and edges. In fig. 6a traces of edges appear as discontinuities in first order directional derivatives, whereas fig. 6b is smooth over the edges.

outer edges well, but pull the surface away from the inner edge. In contrast to the angle ratio method of eq. (8), which considers only a single ERBS surface patch, the modified ERBS triangle method in eqs. (6) and (7) approximates edges better since evaluations from outer patch edges are blended in. Visual examples showing the difference between the two blending functions applied to a synthetic TIN are provided in figs. 6a and 6b.

Another consequence of the ERBS Hermite interpolation properties is that the construction will work even for higher order derivatives than the bi-linear Bézier case considered here, since all existing derivatives from the underlying local patches are propagated to the ERBS surface patches. The method will still be local within the second neighborhood, given that information regarding derivatives of higher order is provided with the TIN.

References

[1] D.S. Broomhead, David Lowe, Multivariable functional interpolation and adaptive networks, *Complex Systems*, **2**, No. 3 (1988), 321-355.

[2] Lubomir T. Dechevsky, Arne Lakså, Børre Bang, Expo-rational b-splines, *International Journal of Pure and Applied Mathematics*, **27**, No. 3 (2006), 319-362.

[3] Gerald Farin, Triangular bernstein-bézier patches, *Computer Aided Geometric Design*, **3**, No. 2 (1986), 83-127.

[4] Michael S. Floater, Parametrization and smooth approximation of surface triangulations, *Computer Aided Geometric Design*, **14**, No. 3 (1997), 231-250.

[5] Michael S. Floater, Mean value coordinates, *Computer Aided Geometric Design*, **20**, No. 1 (2003), 19-27.

[6] Ming-Jun Lai, Larry L. Schumaker, *Spline Functions on Triangulations*, *Encyclopedia of Mathematics and Its Applications*, Cambridge University Press, Cambridge CB2 8RU, UK, **110** (2007).

[7] A. Lakså, *Basic Properties of Expo-Rational B-Splines and Practical Use in Computer Aided Geometric Design*, PhD Thesis, University of Oslo (2007).

[8] A. Lakså, B. Bang, L.T. Dechevsky, Exploring expo-rational b-splines for curves and surfaces, In: *Mathematical methods for Curves and Surfaces* (Ed-s: M. Dæhlen, K. Mørken, L. Schumaker), Nashboro Press (2005), 253-262.

[9] Robert Laurini, Derek Thompson, *Fundamentals of Spatial Information Systems*, In: A.P.I.C. Academic Press, **37** (1992), 24-28, Oval Road, London, NW17DX.

[10] Thomas K. Peucker, Robert J. Fowler, James J. Little, David M. Mark, The triangulated irregular network, In: *Proceedings of Auto Carto*, **4**, No. 2 (1978), 96-103, Reston, Virginia, USA.

[11] Thomas K. Peucker, Robert J. Fowler, James J. Little, David M. Mark, The triangulated irregular network, In: *Proceedings of American Society of Photogrammetry: Digital Terrain Models (DTM) Symposium*, St. Louis, Missouri, USA (1978), 516-540.

[12] Larry L. Schumaker, Tatyana Sorokina, Smooth macro-elements on powell-sabin-12 splits, *Mathematics of Computation*, **75**, No. 254 (2006), 711-726.